

Self-Replicating Molecules: A Second Generation

Edward A. Wintner, M. Morgan Conn, and Julius Rebek, Jr.*

Contribution from the Department of Chemistry, Massachusetts Institute of Technology, Cambridge, Massachusetts 02139

Received January 24, 1994[Ⓞ]

Abstract: The use of self-complementary structures in replication experiments is discussed, and a second generation of self-replicating molecules is introduced. Key design elements of the new system are described, specifically a high affinity ($K_a \sim 10^5 \text{ M}^{-1}$ in CDCl_3) between the two complementary reactive components and the careful placement of nucleophilic and electrophilic centers within the system. These considerations preclude intramolecular reactions within two-component complexes, thus minimizing undesirable background reactions. Autocatalysis is observed in the new systems, and by using appropriate control experiments the autocatalysis is traced to template effects.

Introduction

Previous studies from these laboratories have shown how simple organic structures can catalyze their own formation.^{1,2} Self-complementarity is the key to this autocatalytic behavior; by complementary it is meant that the sizes, shapes, and chemical surfaces of the structures are arranged so as to have affinity for each other. The affinity arises from weak, intermolecular forces—hydrogen bonding and aryl stacking interactions—that act on molecular surfaces. These forces gather the reaction components and anchor them on the template surface while the intracomplex reaction takes place. The process leads to replication of the template, and the molecules are called replicators.

Template effects, leading to reduced activation entropies, are responsible for the autocatalysis observed in our replicators, in nucleic acid replicators,³ in bisubstrate reaction systems,⁴ and in a number of other processes.⁵ It has been our goal to enhance the template process relative to the more random background reactions. Chemical catalysis—positioning acids and bases on the template surface—is one means to this goal; such functions could be trained on the reactant transition states while the reactants were held to the template. In the present study, however, we introduce an alternative tactic: reduce the rate of background reactions.

Molecular replication is simply an autocatalytic reaction where the product of a chemical transformation acts to catalyze that transformation through the *directed* production of copies of the molecule. Model studies of self-replication focus on two types of autocatalytic systems: (1) replication of physical entities and (2) replication of template-based structures. The replication of physical entities is exemplified by the autocatalytic generation of micelles in a system developed by Luisi.^{6,7} Replication of template based structures, as explored in our laboratory and others,^{8,9} has been achieved through the creation of self-complementary molecules.

* Address correspondence to this author at the Massachusetts Institute of Technology.

Ⓞ Abstract published in *Advance ACS Abstracts*, September 1, 1994.

- (1) Rebek, J., Jr. *Chem. Ind.* **1992**, 171-174.
- (2) Wintner, E. A.; Conn, M. M.; Rebek, J., Jr. *Acc. Chem. Res.* **1994**, *27*, 198-203.
- (3) Orgel, L. E. *Nature* **1992**, *358*, 203-209.
- (4) Kelly, T. R.; Bridger, G. J.; Zhao, C. *J. Am. Chem. Soc.* **1990**, *112*, 8024-8034.
- (5) Anderson, S.; Anderson, H. L.; Sanders, J. K. M. *Acc. Chem. Res.* **1991**, *26*, 469-475.
- (6) Bachmann, P. A.; Luisi, P. L.; Lang, J. *Nature* **1992**, *357*, 57-59.
- (7) Bachmann, P. A.; Walde, P.; Luisi, P. L.; Lang, J. *J. Am. Chem. Soc.* **1991**, *113*, 8204-8209.
- (8) von Kiedrowski, G. *Angew. Chem. Int. Ed. Engl.* **1986**, *25*, 932-935.
- (9) von Kiedrowski, G.; Wlotzka, B.; Helbing, J.; Matzen, M.; Jordan, S. *Angew. Chem. Int. Ed. Engl.* **1991**, *30*, 423-426.

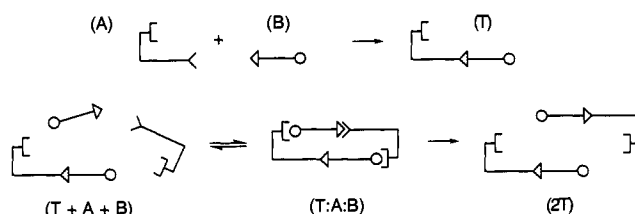


Figure 1. Schematic of self-complementary template-based autocatalysis.

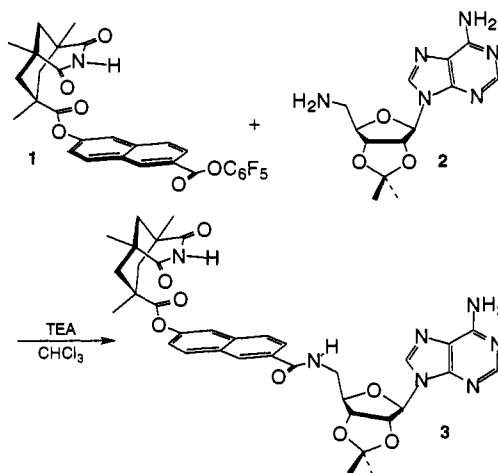


Figure 2. An abiotic self-replicating system.

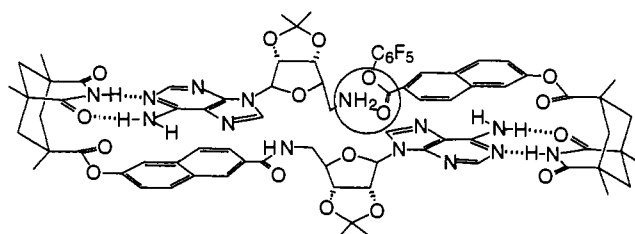


Figure 3. Proposed termolecular complex 3-2-1.

Self-complementary autocatalysis relies on an efficient reaction within a termolecular complex. As shown in Figure 1, two complementary components A and B react in an intermolecular fashion to form template T. Due to the self-complementary nature of the template, two additional units of A and B form a termolecular complex with the template T:A:B. Intracomplex reaction produces the dimer 2T, which dissociates and repeats the process. Ideally, some form of chemical catalysis occurs in

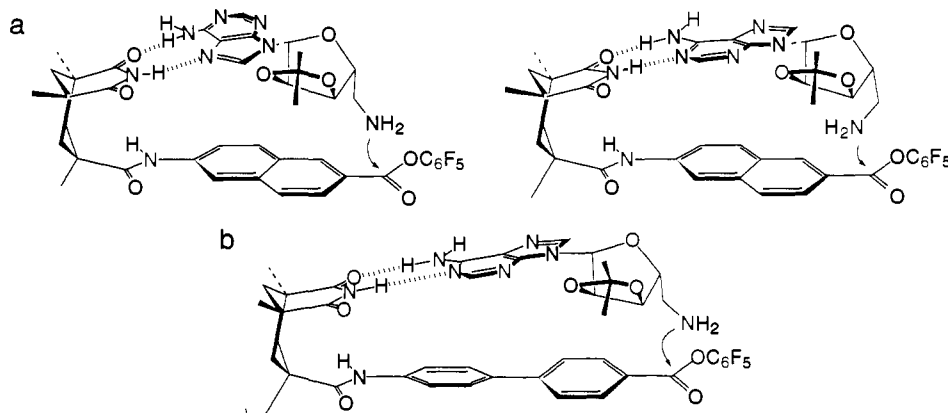


Figure 4. (a) Hoogsteen- and Watson-Crick-type intracomplex reactions in the naphthyl self-replicating system. (b) Intracomplex reaction in the biphenyl self-replicating system.

the termolecular complex, but typically rate enhancement is derived primarily from the reduction in entropy caused by bringing together the reagents on a template.

In the laboratory, self-complementary autocatalysis was first realized with DNA. Von Kiedrowski showed that complementary trioxynucleotides CCG and CGG could be coupled in the presence of a water-soluble condensation agent to form the self-complementary hexadeoxynucleotide by an autocatalytic process.⁸ Subsequent improvements were made in the efficiency of autocatalysis; greater efficiency led to parabolic growth in the hexadeoxynucleotide concentration, reflecting the exponential nature of an autocatalytic process.⁹

Synthetic Replicators. Our first abiotic self-replicating system was based on the hydrogen-bonding recognition of adenine and a Kemp's triacid imide.¹⁰ Naphthoyl active ester **1** was reacted with 5'-amino-5'-deoxy-2',3'-isopropylideneadenosine (**2**) to form self-complementary autocatalytic template **3** (Figure 2). While the catalytic efficiency within the termolecular complex was too low to observe exponential growth of the template, the autocatalytic nature of the reaction was evident from the rate acceleration caused by seeding the reaction with its product **3**. It is significant that substitution of a methyl group for the imide hydrogen of **3** led to a molecule which was not a catalyst for the reaction of **1** and **2**; molecular recognition was required for replication.¹¹ Our results thus indicated template-catalyzed replication as the source of autocatalysis, where recognition surfaces and functional groups interact to form a productive termolecular complex as proposed in Figure 3.

One of the complications of this naphthyl system was that in both Hoogsteen and Watson-Crick binding modes, coupling between the amine and ester could occur within a complex of the two precursors (Figure 4a). The initial product of this bimolecular pre-associative mechanism was postulated to be a *cis*-amide, which isomerized to the *trans*-amide, the active form of the template. In fact, this appears to be the major background pathway for product formation.¹¹ By changing the spacer element in this molecule from a 2,6-naphthyl to a 4,4'-biphenyl, the ester and amine were moved away from each other.¹² Intracomplex reaction could now occur only if the adenosine were bound in the more-extended Watson-Crick mode as shown in Figure 4b. By reducing the amount of preassociative catalysis, the effect of the autocatalytic pathway was seen as a gentle sigmoidality in the initial rate of growth of product.¹² This result was further exploited for a study of molecular competition and "mutation" using *N*⁶-CBZ derivatives of adenosine.¹³

The Second Generation. Given that there exist several reaction channels to product in the naphthyl and biphenyl replicators, one way to force the reaction to the template-catalyzed mechanism is to restrain the preassociative bimolecular pathway. The spacer element in the receptor must be of sufficient length to keep the amine and ester groups from reacting in a bimolecular complex, regardless of the binding mode of adenine, and yet the affinity of the components for each other must be high. Alternatively stated, the complex must have a large K_a and must position the components unambiguously.

These criteria can be fulfilled by a diaminocarbazole-based diimide module such as **11**, a nearly ideal complement to the purine nucleus of adenine.¹⁴⁻¹⁶ The imides can chelate the purine through simultaneous Watson-Crick and Hoogsteen base-pairing, and the extended heterocyclic surface of the carbazole can stack against the purine. Not only is the binding affinity for adenosine derivatives extremely high ($K_a \sim 10^5 \text{ M}^{-1}$ in CDCl_3), but with triplex-like chelation of the adenine moiety,¹⁶ conformational complications from the switching of bound adenine between Watson-Crick and Hoogsteen binding modes are eliminated. Furthermore, a biphenyl substituent on *N*⁹ of the carbazole diimide can eliminate any preassociative bimolecular reactions (such as those in Figures 4a,b) by enforcing the separation of ester and bound amine. Precise positioning of the two complementary components is thus achieved in the system.

Figure 5 shows the computer-predicted geometry of a bimolecular complex between **2** and the biphenylcarbazole diimide **9**. From the figure, it is clear that the amine and ester are separated by a significant distance, $>5.5 \text{ \AA}$ in the computer-generated model. This distance is well defined, as the diimide-bound adenine has only limited motion within the complex. Since the two reactive centers cannot approach each other within the complex, a bimolecular preassociative pathway is ruled out. Reaction of **2** + **11** to form the self-complementary template molecule **12** must occur either in an unassisted intermolecular fashion or through the template catalyzed complex **12**·**11**·**2**.

Synthesis. Synthesis of the biphenyl derivative began with 4'-iodobiphenyl-4-carboxylic acid (**4**) and proceeded through Ullmann coupling¹⁷ of methyl 4'-iodobiphenyl-4-carboxylate (**5**) and carbazole to give **6** (Scheme 1). Nitration to the dinitro **7** followed by reduction ($\text{H}_2/\text{Pd-C}$, THF) gave the amine **8**, and subsequent condensation with the tripropyl derivative of Kemp's

(13) Hong, J.-I.; Feng, Q.; Rotello, V.; Rebek, J., Jr. *Science* **1992**, *255*, 848-850.

(14) Galán, A.; de Mendoza, J.; Toiron, C.; Bruix, M.; Deslongchamps, G.; Rebek, J., Jr. *J. Am. Chem. Soc.* **1991**, *113*, 9424-9425.

(15) Deslongchamps, G.; Galán, A.; de Mendoza, J.; Rebek, J., Jr. *Angew. Chem. Int. Ed. Engl.* **1992**, *31*, 61-63.

(16) Conn, M. M.; Wintner, E. A.; Rebek, J., Jr. *Angew. Chem., Int. Ed. Engl.* **1994**, *33*, 1577-1579. Conn, M. M.; Deslongchamps, G.; de Mendoza, J.; Rebek, J., Jr. *J. Am. Chem. Soc.* **1993**, *115*, 3548-3557.

(17) For a review, see Lindley, J. *Tetrahedron* **1984**, *40*, 1433-1456.

(10) Tjivikua, T.; Ballester, P.; Rebek, J., Jr. *J. Am. Chem. Soc.* **1990**, *112*, 1249-1250.

(11) Nowick, J. S.; Feng, Q.; Tjivikua, T.; Ballester, P.; Rebek, J., Jr. *J. Am. Chem. Soc.* **1991**, *113*, 8831-8839.

(12) Rotello, V.; Hong, J. I.; Rebek, J., Jr. *J. Am. Chem. Soc.* **1991**, *113*, 9422-9423.

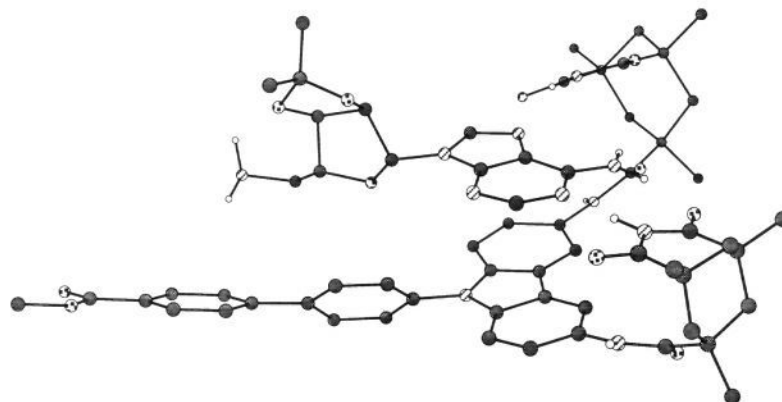
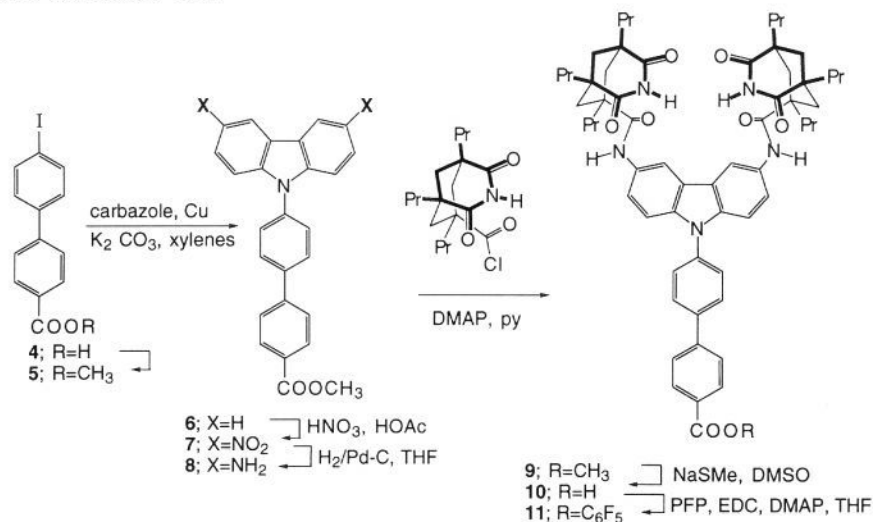


Figure 5. Computer-generated complex between the biphenylcarbazole **9** and aminoadenosine **2**.

Scheme 1. Synthesis of the Diimide Cleft



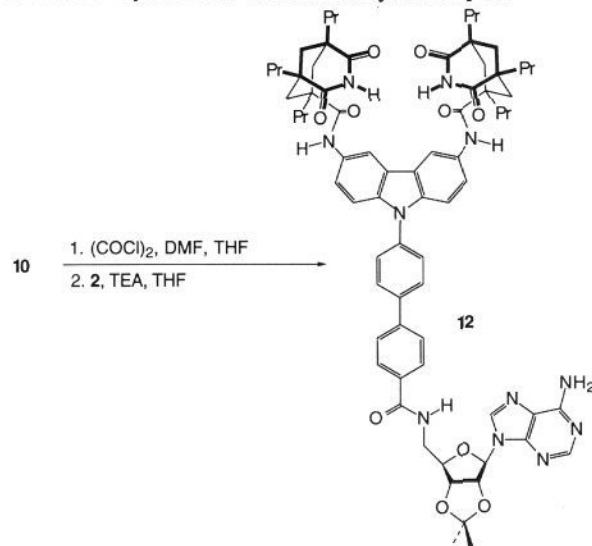
triacid as the imide acid chloride¹⁸ yielded the methyl ester **9**. Demethylation of **9** was achieved by S_N2 dealkylation with thiolate anion.¹⁹ The pentafluorophenyl ester **11** was prepared by EDC coupling of acid **10** and excess pentafluorophenol (PFP) in THF, with catalytic DMAP. Condensation of the corresponding acid chloride of **10** (oxalyl chloride) with adenosine **2** produced the amide **12** (Scheme 2).

Results and Discussion

The biphenylcarbazole diimide structure provides very high affinity for 2',3'-isopropylideneadenosine. As the slow exchange of the molecule leads to highly broadened ¹H NMR spectra during titration, the binding constant in CDCl₃ can only be estimated as 10⁵ M⁻¹. The components are readily soluble in THF, and the association constant between **9** and 2',3'-isopropylideneadenosine was measured by ¹H NMR titration in THF-*d*₆ to be 576 M⁻¹ at 298 K based on the downfield shift of the imide proton from 9.65 to 12.87 ppm.

With an association constant on the order of 10⁵ M⁻¹ in chloroform, the dimerization constant can be crudely estimated to be on the order of 10¹⁰ M⁻¹ (K_a^2); in the absence of either negative or positive cooperativity, the dimerization interaction energy will be at least the sum of two individual association energies.²⁰ The second binding event in dimerization should be favored by the fact that the translational and some intermolecular

Scheme 2. Synthesis of the Autocatalytic Template



rotational entropy between the two molecules has already been overcome, though internal strain could reduce dimerization.

Variable-temperature ¹H NMR spectra for a 5 mM solution (CDCl₃) of the self-complementary **12** show two sharp imide peaks centered at 13 ppm at -55 °C (Figure 6). The inherent asymmetry of the chelated adenine causes the chemical environments of the Watson-Crick and Hoogsteen binding modes to

(18) Jeong, K. S.; Muehldorf, A. V.; Rebek, J., Jr. *J. Am. Chem. Soc.* **1990**, *112*, 6144-6145.

(19) For a review, see McMurry, J. *Org. React.* **1976**, *24*, 187-224.

(20) Breslow, R.; Halfon, S. *Proc. Natl. Acad. Sci. U.S.A.* **1992**, *89*, 6916-6918.

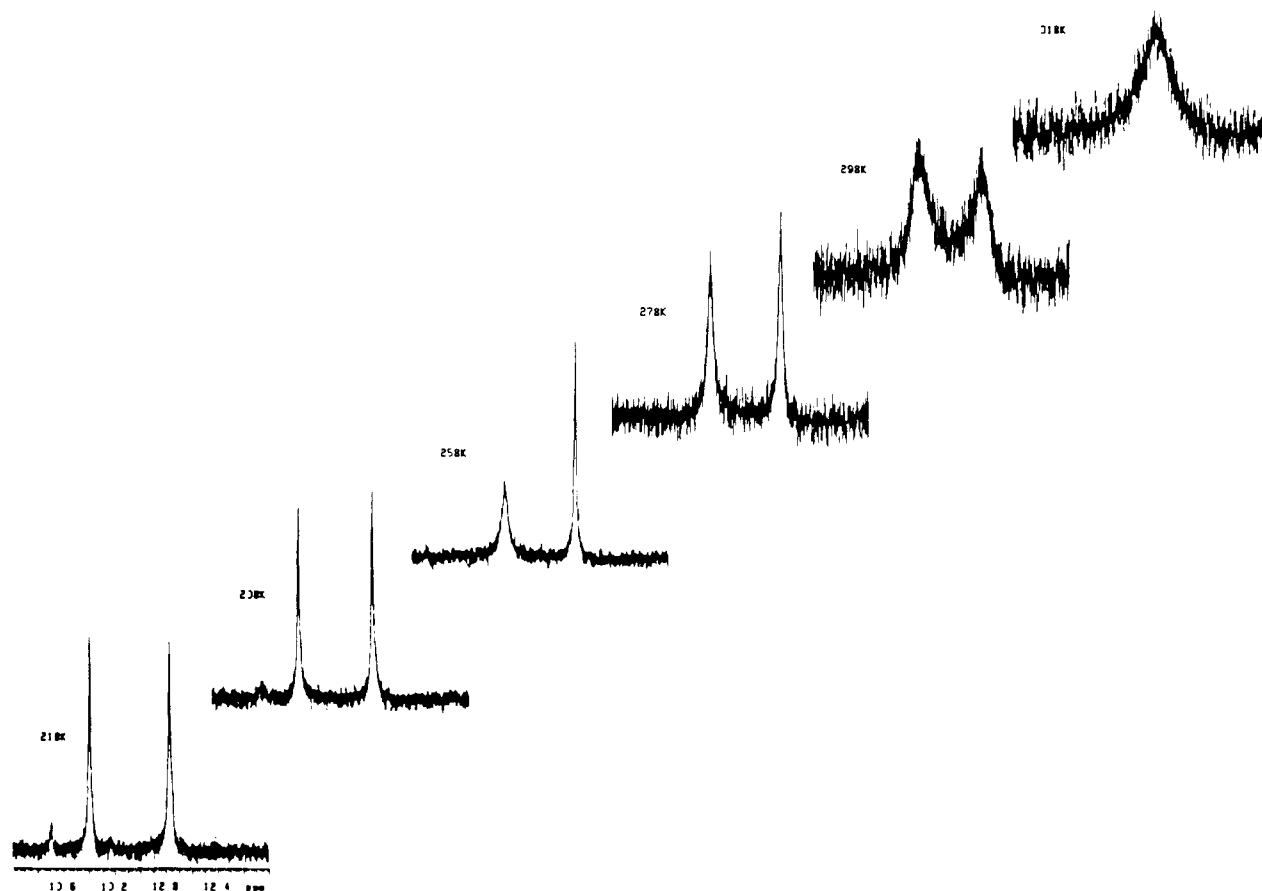


Figure 6. Variation of the imide region of the ^1H NMR spectrum of **12** with temperature (CDCl_3).

differ, giving rise to two different imide chemical shifts when exchange is slowed.¹⁶ Two-dimensional NOESY studies of a related carbazole-bis(imide)¹⁶ at low temperature suggest that the downfield imide proton forms the Hoogsteen bond.²¹ The shape of the adenine-bis(imide) complex mandates that the hydrogen bonds on either side of the purine be of unequal length, and this is reflected in the different responses of the two imide shifts to temperature change. The imide resonances begin to broaden at -25°C , with more broadening of the downfield imide, and coalesce to a single broad resonance between 35 and 45°C . With a maximum $\Delta\nu$ of 311 Hz (-55°C), standard dynamic NMR theory²² gives a barrier to conversion between the two imides at the coalescence temperature (taken to be 40°C) of approximately 14.3 kcal/mol . Since no other binding modes are likely, this behavior can be considered the paradigm for a purely dimeric system.

In $\text{THF-}d_8$, the dimerization constant is expected to be in the vicinity of $3 \times 10^5\text{ M}^{-1}$. While there is concentration dependence in the ^1H NMR spectrum of **12** in $\text{THF-}d_8$ from 0.057 to 5.081 mM , broadening of the resonances makes it impossible to calculate a dimerization constant. The dimerization of **12** appears so strong, in fact, that dimerization occurs even in DMSO, despite the highly competitive nature of this solvent for hydrogen bonding sites. A dimerization constant of 169 M^{-1} was calculated based on ^1H NMR dilution studies in $\text{DMSO-}d_6$ (0.068 – 6.13 mM).

Kinetic studies of the coupling reaction (Figure 7) were performed in CHCl_3 -THF mixtures using the pentafluorophenyl active ester **11** and the amine **2**. Product appearance of the amide product **12** was followed by HPLC. The results are summarized in Figure 9 and Table 1 and reveal the following:

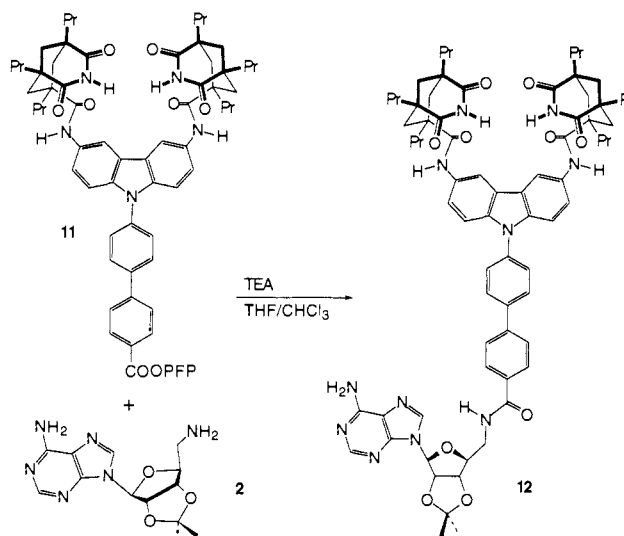


Figure 7. The autocatalytic reaction.

(1) Autocatalysis occurs in the complementary system. Addition of the product **12** increases the rate of the coupling reaction of the ester **11** with **2**. Experiments at 6.2 mM show a 54% increase in initial rate with 0.5 equiv of added **12** (Figure 9, Table 1). This enhancement is comparable to that observed with our original replicators.¹⁰

(2) The imide function alone is not the source of the autocatalysis. This was established by control experiments with the diimide methyl ester **9** (Scheme 1). This molecule does not catalyze the reaction of **11** with **2**; rather, inhibition results, probably as a consequence of its sequestering the aminoadenosine in an unproductive complex. Additional experiments with **13**

(21) Conn, M. M. Ph.D. Thesis. Massachusetts Institute of Technology. Feb, 1994.

(22) Sandström, J. *Dynamic NMR Spectroscopy*; Academic Press: London, 1982.

Table 1. Generation of Product 12 as a Function of Time

reaction	additive	individual initial rates of product formation ($\mu\text{M}/\text{min}$)								avg initial rate of product formation ($\mu\text{M}/\text{min}$)	
		1.72	1.77	1.63	1.69	1.74	1.63	1.80	1.72		relative rate
a	nothing									1.71 ± 0.06	1.00
b	product 12 (0.5 equiv)	2.75	2.60	2.49	2.68					2.63 ± 0.11	1.54 ± 0.08
c	imide 13 (0.5 equiv)	1.73	1.71	1.70	1.75					1.72 ± 0.02	1.01 ± 0.04
d	amide 14 (1.0 equiv)	1.44	1.58	1.60	1.63					1.56 ± 0.08	0.91 ± 0.06
e	diimide 9 (0.5 equiv)	1.26	1.05	1.15	1.27					1.18 ± 0.10	0.69 ± 0.06

^a All reactions were performed at 6.2 mM initial concentrations of reactants 2 and 11 in 13% CHCl_3/THF with 1.0% TEA base added, 22 ± 1 °C.

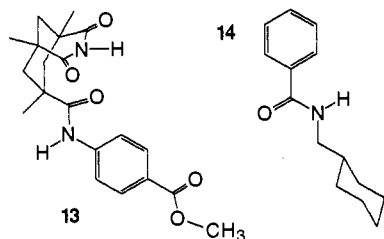


Figure 8.

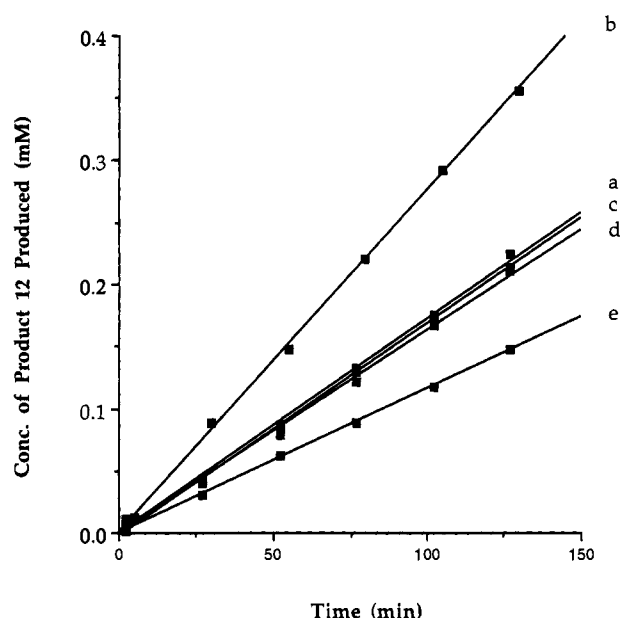


Figure 9. Representative kinetic plots of the generation of product 12 as a function of time (initial 5% of reaction). All reactions were performed at 6.2 mM initial concentrations of reactants 2 and 11 in 13% THF/ CHCl_3 with 1.0% TEA base added, 22 ± 1 °C. All individual slopes (reaction rates) are given in Table 1. (a) Baseline reaction (2 + 11); (b) baseline reaction plus 0.5 equiv of product (12); (c) baseline reaction plus 0.5 equiv of imide methyl ester 13; (d) baseline reaction plus 1.0 equiv of amide 14; (e) baseline reaction plus 0.5 equiv of diimide methyl ester 9.

(Figure 8), which competes only poorly for adenosines, further support the conclusion that the imide is an ineffective catalyst.

(3) The naphthoyl amide does not catalyze the reaction. The coupling rate of 11 with 2 is not increased by the addition of the benzoyl derivative 14 (Figure 8), which presents a secondary amide function in a steric environment similar to the one in 12, but lacks recognition elements. This result is consistent with results in other self-replicating systems involving adenine recognition.¹⁰⁻¹²

(4) Previous control experiments with adenosines (9-ethyladenine and the *N*-methyl derivative of the imide 3) have shown that neither the purine nor the ribose are effective as catalysts for an acylation reaction.^{2,11} (This result is further supported by the data in Table 2, *q.v.*)

(5) Self-replication is the result. Separated, the individual features and functionalities of 12 are unable to account for the

autocatalysis observed. Instead, the effect of the whole molecule is greater than the sum of its parts. The most economical explanation for the autocatalytic nature of 12 is that the molecule serves as a template for its own replication: the initial reaction to form 12 is relatively slow, but once present, it can form a productive termolecular complex, 12·11·2 held together by complementary recognition surfaces. Within the complex, functional groups are presented in such a way that the transition state of the tetrahedral intermediate (modeled in Figure 10 as the neutral tautomer) is easily reached.

In further control experiments, we found that under these conditions, autocatalysis is not a general feature of ester aminolysis. Parallel experiments with the naphthyl ester 15 and amine 2 (Figure 11) show that within experimental error, the amide product 16 does not significantly catalyze its own formation (Table 2). Interestingly, complexation of 2 with the diimide methyl ester 9 inhibits the reaction of 2 with 15 just as it does the reaction of 2 with 11. In both cases, the inhibition is presumably due to the ability of the diimide 9 to sequester 2 in an unproductive complex.

What are the consequences of complexation for replicators? The rate of formation of 12 compared with that of 16 under identical conditions reveals that recognition slows the rate of coupling by a factor of two; in the presence of 2, pentafluorophenyl ester species which are unable to complex 2 (*e.g.* 15) are twice as reactive toward amines than is ester 11. For the same reasons, however, noncomplexed esters are also more exposed to side reactions. Structures which recognize each other and form complexes become stabilized; the surfaces in contact are protected from external, often harmful reagents, and the protected structures react primarily with molecules which are specifically complexed with them.²³ Accordingly, molecular recognition offers advantages for evolution at the molecular level; survival as well as replication is enhanced.

The exact nature of complexation in a self-replicating system is critical, and eventually it would be optimal to construct a template which binds more tightly to the transition state of its formation than to itself. While the present template 12 binds its components 2 and 11 far more strongly than its predecessors (*e.g.* 3), it suffers from extreme product inhibition through dimerization. The catalytic efficiency of the template 12 should be excellent given the binding affinities within a termolecular complex of 12, 11, and 2, but even a very crude estimate of the concentration of template monomer in reaction b (on the order of 1 μM)²⁴ shows that dimerization detracts severely from the effectiveness of 12 as a replicator. That so little template gives rise to a 54% increase in rate indicates the success of 12 in positioning its substrates for reaction. If such molecular recognition could be

(23) There are earlier examples of a template slowing down a reaction but improving the yield of the desired molecule; see Dietrich-Buchecker, Ch., Sauvage, J. P. *New J. Chem.* 1992, 16, 277-285.

(24) Concentration of template monomer at 3.1 mM total template concentration (reaction b, 0.5 equiv of template added) was calculated by estimating a single binding event at $86\,000\text{ M}^{-1}$ in 13% THF/ CHCl_3 (between 576 and 10^5 M^{-1}) and taking the dimerization of the template to be the square of that value. Values were inserted into a model of autocatalysis developed by James Nowick (see details in ref 11). Concentration of template monomer may also be approximated using $K_{\text{dim}} = [\text{template dimer}]/[\text{template monomer}]^2$.

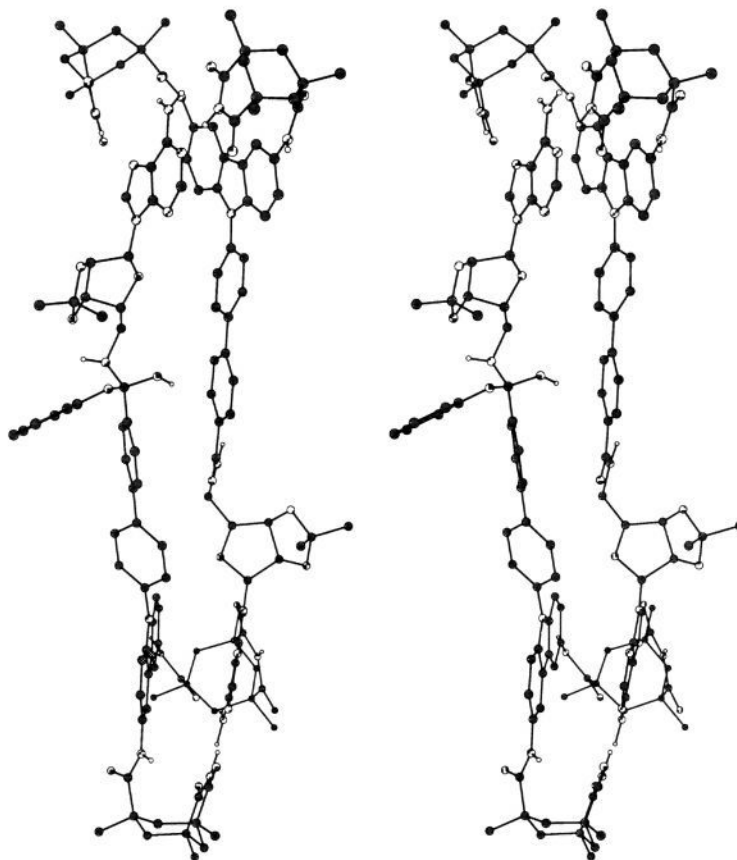


Figure 10. Predicted structure for the autocatalytic tetrahedral intermediate of the complex **12-11-2** (stereo view). Hydrogens attached to carbon have been omitted for clarity.

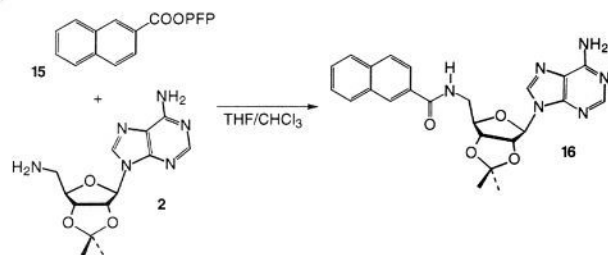


Figure 11. A nonreplicating control system.

Table 2. Generation of Product **16** as a Function of Time

additive	individual initial rates of product formation ($\mu\text{M}/\text{min}$)			avg initial rate of product formation ($\mu\text{M}/\text{min}$)	relative rate
nothing	3.76	3.84	3.73	3.78 ± 0.06	1.00
amide 16 (0.5 equiv)	4.11	4.05	4.07	4.08 ± 0.03	1.08 ± 0.02
diimide 9 (1 equiv)	2.32	2.64	2.85	2.60 ± 0.27	0.69 ± 0.07

^a All reactions were performed at 6.2 mM initial concentrations of reactants **2** and **15** in 13% CHCl_3/THF with 1.0% TEA base added, 22 ± 1 °C.

trained on the transition state of the reaction at the expense of the ground state dimer, a new level of self replication might be achieved.

For now, our targets are much more modest molecules in which functional groups are incorporated into the template for *chemical catalysis* of the replication step.²⁵ These include functionalities which can enhance proton transfers within the tetrahedral

intermediates formed and destroyed along the coupling pathway. In addition, the new high-affinity molecules augur well for the synthesis of structures capable of replication in aqueous media. We will report on these in due course.

Experimental Section

Synthesis. General. All commercially available compounds (Aldrich) were used without further purification unless otherwise indicated. DMSO-*d*₆ (99.9%-D, MSD Isotopes or Cambridge Isotope Labs) were used from freshly opened vials. CDCl_3 (99.8%-D, MSD or CIL) was stored over molecular sieves and passed through dry basic alumina just prior to use. Tetrahydrofuran used in anhydrous conditions were distilled from sodium-benzophenone ketyl; dimethyl sulfoxide was distilled from sodium hydroxide and stored over molecular sieves (4 Å). Thin layer chromatography was performed on Merck Silica 60 F-254 precoated TLC plates. Column chromatography was performed on Merck Silica Gel 60 (230–400 mesh) according to Still *et al.*²⁶ Glassware used for anhydrous conditions either was baked overnight at 150 °C, assembled hot, cooled under vacuum, and filled with argon, or was flamed dry under vacuum, cooled, and filled with argon before use. Standard inert-atmosphere techniques were used for solvent transfers by syringe. All reagents were supplied by the Aldrich Chemical Co. 5'-Amino-5'-deoxy-2',3'-isopropylideneadenosine (**2**) was synthesized according to Kolb *et al.*²⁷

¹H NMR spectra were recorded on Varian XL-300, UN-300, and VXR-500 spectrometers in solvents as indicated. Chemical shifts are reported as parts per million (δ) relative to residual solvent protons. Melting points were obtained on an Electrothermal IA9100 digital melting point apparatus and are calibrated. IR spectra were recorded on a Perkin-Elmer series 1600 FT-IR spectrometer. High resolution mass spectra were obtained on a Finnegan MAT 8200 mass spectrometer.

(26) Still, W. C.; Kahn, M.; Mitra, A. *J. Org. Chem.* **1978**, *43*, 2923–2925.

(27) Kolb, M.; Danzin, C.; Barth, J.; Claverie, N. *J. Med. Chem.* **1982**, *25*, 550–556.

(25) Andreu, C.; Beerli, R.; Branda, N.; Conn, M. M.; de Mendoza, J.; Galán, A.; Huc, I.; Kato, Y.; Tymoschenko, M.; Valdez, C.; Wintner, E.; Wyler, R.; Rebek, J. Jr. *Pure Appl. Chem.* **1993**, *65*, 2313–2318.

4'-Iodo-4-biphenylcarboxylic Acid (4). Iodination of 4-biphenylcarboxylic acid was performed according to Merkushev and Yudina.²⁸

Methyl 4'-Iodo-4-biphenylcarboxylate (5). Thionyl chloride (50 mL) was added slowly dropwise over 2 h to a suspension of acid **4** (14.49 g, 44.707 mmol) in dry MeOH under a drying tube. The suspension was refluxed for 4 h and stirred at room temperature for 24 h. Solvents were removed by rotary evaporation and then under vacuum. The crude was recrystallized from refluxing EtOAc (100 mL) and CHCl₃ (200 mL) to give 10.63 g (70%) of off-white platelets: ¹H NMR (500 MHz, CDCl₃) δ 8.102 (d, 2 H, *J* = 8.5 Hz), 7.796 (d, 2 H, *J* = 8.8 Hz), 7.617 (d, 2 H, *J* = 8.5 Hz), 7.356 (d, 2 H, *J* = 8.5 Hz), 3.943 (s, 3 H).

N-(4-(4-(Methoxycarbonyl)phenyl)phenyl)carbazole (6). Iodobiphenyl **5** (5.26 g, 31.43 mmol), carbazole (1.001 equiv), K₂CO₃ (1.001 equiv), and Cu powder (0.127 equiv) were intimately mixed with mortar and pestle. The solids were suspended in xylenes (20 mL) and mechanically stirred under reflux for 2 days. The reaction was slightly cooled and then briefly refluxed with benzene (250 mL). The suspension was cooled, stirred overnight, filtered through Celite, and reduced by rotary evaporation under reduced pressure. The residue was recrystallized from refluxing MeOH (50 mL) and EtOAc (200 mL) to give 5 g of off-white flaky crystals. The mother liquor was concentrated and again recrystallized from refluxing MeOH (30 mL) and EtOAc (60 mL) to give 1.11 g of product. The second mother liquor was concentrated and purified by chromatography (50% hexanes/CHCl₃) to give 269 mg of pure product. The combined yield of crystalline **6** was 6.379 g (54%): mp 191.7–192.7 °C; IR (KBr) 2949, 1721, 1604, 1528, 1496, 1450, 1276, 1230, 1178, 1110, 835, 774, 753, 724 cm⁻¹; ¹H NMR (300 MHz, CDCl₃) δ 8.181 (d, 2 H, *J* = 8.6 Hz), 8.169 (d, 2 H, *J* = 7.5 Hz), 7.864 (d, 2 H, *J* = 8.6 Hz), 7.770 (d, 2 H, *J* = 8.6 Hz), 7.684 (d, 2 H, *J* = 8.8 Hz), 7.489 (d, 2 H, *J* = 7.7 Hz), 7.439 (td, 2 H, *J* = 7.5, 1.2 Hz), 7.315 (m, 2 H), 3.976 (s, 3 H); HRMS (EI) calcd for C₂₆H₁₉NO₂ 377.1416, found 377.1416.

N-(4-(4-(Methoxycarbonyl)phenyl)phenyl)-3,6-dinitrocarbazole (7). Carbazole **6** (3.03 g, 8.03 mmol) was suspended in HOAc (60 mL) and brought to 70 °C in an oil bath. HNO₃ (concd, 30 mL) was added dropwise over 0.5 h under a drying tube. The yellow suspension was stirred at this temperature for 5 h and brought to room temperature for 3 h. The suspension was stirred with water (200 mL), filtered, and dried to give 3.635 g (97%) of yellow powder **7** which was used without further purification: ¹H NMR (500 MHz, DMSO-*d*₆) δ 9.642 (d, 2 H, *J* = 2.5 Hz), 8.419 (dd, 2 H, *J* = 9.5, 2.5 Hz), 8.116 (d, 2 H, *J* = 8.5 Hz), 8.103 (d, 2 H, *J* = 8.0 Hz), 7.984 (d, 2 H, *J* = 8.5 Hz), 7.860 (d, 2 H, *J* = 8.5 Hz), 7.605 (d, 2 H, *J* = 9.5 Hz), 3.896 (s, 3 H).

N-(4-(4-(Methoxycarbonyl)phenyl)phenyl)-3,6-diaminocarbazole (8). A suspension of dinitro **7** (887 mg, 1.897 mmol) and 10% Pd-C (22 wt %) in THF (150 mL) was hydrogenated at balloon pressure for 26 h. After filtration through Celite, solvent was removed by rotary evaporation and the unstable yellow solid was carried on immediately: ¹H NMR (500 MHz, CDCl₃) δ 8.157 (d, 2 H, *J* = 8.5 Hz), 7.801 (d, 2 H, *J* = 9.0 Hz), 7.744 (d, 2 H, *J* = 8.5 Hz), 7.651 (d, 2 H, *J* = 9.0 Hz), 7.333 (d, 2 H, *J* = 8.5 Hz), 7.277 (d, 2 H, *J* = 2.5 Hz), 6.986 (s, 2 H, amine), 6.767 (dd, 2 H, *J* = 8.7, 2.2 Hz), 3.98 (s, 3 H).

N-(4-(4-(Methoxycarbonyl)phenyl)phenyl)-3,6-bis((*cis,cis*-2,4-dioxo-1,5,7-tripropyl-3-azabicyclo[3.3.1]non-7-yl)carbonyl)amino)carbazole (9). Diamine **8** and tripropyl Kempf's acyl chloride¹⁸ (2.05 mol equiv) were refluxed with catalytic DMAP (0.1 equiv) in pyridine (50 mL) for 16 h under Ar. Solvent was removed by rotary evaporation under reduced pressure and the residue taken up in EtOAc (200 mL) and CHCl₃ (25 mL). The combined organic layers were washed with 1 N HCl (40 mL) and brine (50 mL) and dried over Na₂SO₄. After concentration, the crude product was purified by gravity chromatography (2.5% MeOH/CHCl₃), followed by trituration in MeOH (20 mL). The yellowish solid was trituated a second time in MeOH (20 mL) to give 1.129 g (58%) of beige solid: IR (KBr) 3378, 3210, 2958, 1700, 1466, 1280, 1198, 1113, 774 cm⁻¹; ¹H NMR (500 MHz, DMSO-*d*₆) δ 10.368 (s, 2 H, imide), 9.232 (s, 2 H, amide), 8.312 (d, 2 H, *J* = 1.7 Hz), 8.096 (d, 2 H, *J* = 8.5 Hz), 8.048 (d, 2 H, *J* = 8.5 Hz), 7.966 (d, 2 H, *J* = 8.5 Hz), 7.738 (d, 2 H, *J* = 8.3 Hz), 7.494 (dd, 2 H, *J* = 9.0, 1.7 Hz), 7.379 (d, 2 H, *J* = 8.8 Hz), 3.892 (s, 3 H), 2.682 (d, 4 H, *J* = 13.9 Hz), 2.031 (d, 2 H, *J* = 12.7 Hz), 1.78 (m, 4 H), 1.51 (m, 4 H), 1.4–1.1 (m, 22 H), 0.876 (t, 12 H, *J* = 7.1 Hz), 0.807 (t, 6 H, *J* = 7.2 Hz); HRMS (FAB in 3-nitrobenzyl alcohol) calcd for C₆₂H₇₆N₅O₈ (M + H) 1018.5694, found 1018.5690.

N-(4-(4-(Carboxyphenyl)phenyl)-3,6-bis((*cis,cis*-2,4-dioxo-1,5,7-tripropyl-3-azabicyclo[3.3.1]non-7-yl)carbonyl)amino)carbazole (10). Anhydrous DMSO (10 mL) was added via syringe to ester **9** (402 mg, 0.3948 mmol) and NaMe (5.2 equiv) under Ar and the pale yellow solution was stirred at 80 °C for 1 h. After cooling to room temperature, the reaction was taken up in CHCl₃ (50 mL), washed with 1 N HCl (2 × 30 mL), water (2 × 50 mL), and brine (50 mL), and dried over Na₂SO₄. Solvent was removed by rotary evaporation. The pale yellow solid was dried under vacuum to give 375 mg (95%) of acid **10** which was used without further purification: ¹H NMR (500 MHz, DMSO-*d*₆) δ 10.365 (s, 2 H, imide), 9.230 (s, 2 H, amide), 8.312 (d, 2 H, *J* = 1.5 Hz), 8.072 (d, 2 H, *J* = 8.5 Hz), 8.036 (d, 2 H, *J* = 8.5 Hz), 7.931 (d, 2 H, *J* = 8.0 Hz), 7.730 (d, 2 H, *J* = 8.0 Hz), 7.491 (dd, 2 H, *J* = 8.5, 2.0 Hz), 7.377 (d, 2 H, *J* = 8.5 Hz), 2.682 (d, 4 H, *J* = 14.0 Hz), 2.030 (d, 2 H, *J* = 12.5 Hz), 1.80 (m, 4 H), 1.51 (m, 4 H), 1.35–1.1 (m, 22 H), 0.874 (t, 12 H, *J* = 7.0 Hz), 0.805 (t, 6 H, *J* = 7.2 Hz).

N-(4-(4-(pentafluorophenoxy)carbonyl)phenyl)phenyl)-3,6-bis((*cis,cis*-2,4-dioxo-1,5,7-tripropyl-3-azabicyclo[3.3.1]non-7-yl)carbonyl)amino)carbazole (11). Anhydrous THF (~5 mL/100 mg acid) was added to a round-bottomed flask with acid **10**, pentafluorophenol (1.7–2.5 equiv), EDC (1.1–2.8 equiv), and DMAP (catalytic). The reaction mixture was stirred overnight at room temperature under Ar. Solvent was removed by rotary evaporation and the residue chromatographed on silica using EtOAc/CH₂Cl₂. Yields were typically 70–85%. Purity was estimated to be >95% by HPLC.

Template 12. Acid **10** (100 mg, 0.0996 mmol) was dissolved in anhydrous THF (7 mL). Oxalyl chloride (50 μL, 5.76 equiv) and catalytic DMF (1 μL) were added. The yellow solution was stirred under Ar at room temperature for 1 h and solvent was removed by rotary evaporation under reduced pressure. The acid chloride was pumped dry for 4 h. Aminoadenosine **2** (1.18 equiv) was added to the reaction vessel, and anhydrous THF (6 mL) was added to dissolve the reagents. Triethylamine (70 μL, 5.04 equiv) was added to the reaction solution accompanied by immediate formation of a white precipitate. After stirring at room temperature under Ar for 20.5 h, the reaction was filtered and solvents removed by rotary evaporation. Flash chromatography (4% MeOH/CHCl₃) gave partially pure product which was precipitated from an acetone solution (1 mL) with hexanes (5 mL) to give 78 mg (53%) of beige solid **12**: IR (KBr) 3374, 3214, 2958, 1696, 1647, 1491, 1465, 1204, 1079 cm⁻¹; ¹H NMR (500 MHz, DMSO-*d*₆) δ 10.380 (s, 2 H, imide), 9.230 (s, 2 H, amide), 8.361 (s, 1 H), 8.318 (s, 1 H), 8.114 (d, 2 H, *J* = 1.5 Hz), 8.032 (d, 2 H, *J* = 8.5 Hz), 7.983 (d, 2 H, *J* = 8.5 Hz), 7.901 (d, 2 H, *J* = 8.5 Hz), 7.720 (d, 2 H, *J* = 8.0 Hz), 7.492 (dd, 2 H, *J* = 9.0, 1.5 Hz), 7.442 (br s, 2 H, amine), 7.373 (d, 2 H, *J* = 8.5 Hz), 6.174 (d, 1 H, *J* = 2.5 Hz), 5.507 (dd, 1 H, *J* = 6.0, 2.5 Hz), 5.086 (dd, 1 H, *J* = 6.2, 3.2 Hz), 4.344 (m, 1 H), 3.567 (m, 2 H), 2.686 (d, 4 H, *J* = 13.5 Hz), 2.030 (d, 2 H, *J* = 12.5 Hz), 1.78 (m, 4 H), 1.540 (s, 3 H), 1.51 (m, 4 H), 1.326 (s, 3 H), 1.35–1.1 (m, 22 H), 0.876 (t, 12 H, *J* = 7.0 Hz), 0.807 (t, 6 H, *J* = 7.0 Hz); HRMS (FAB in 3-nitrobenzyl alcohol) calcd for C₇₄H₉₀N₁₁O₁₀ (M + H) 1292.6872, found 1292.6860.

Methyl 4-(((*cis,cis*-2,4-Dioxo-1,5,7-tripropyl-3-azabicyclo[3.3.1]non-7-yl)carbonyl)amino)benzoate (13). Reaction of methyl 4-aminobenzoate and Kempf's imide acid chloride was performed using previously published methodology²⁹ to give **13** as a white solid: mp 290–295 °C; IR (KBr) 3357, 3189, 3097, 2978, 2930, 1720, 1689, 1596, 1529 cm⁻¹; ¹H NMR (250 MHz, CDCl₃) δ 7.98 (d, 2 H, *J* = 8.7 Hz), 7.52 (d, 2 H, *J* = 8.7 Hz), 7.50 (s, 1 H), 3.90 (s, 3 H), 2.66 (d, 2 H, *J* = 13.7 Hz), 2.04 (d, 1 H, *J* = 13.7 Hz), 1.44 (d, 2 H, *J* = 13.3 Hz), 1.36 (d, 1 H, *J* = 3.8 Hz), 1.33 (s, 3 H), 1.31 (s, 6 H); HRMS (EI) calcd for C₂₀H₂₄N₂O₅ 372.1685, found 372.1683.

N-(Cyclohexylmethyl)benzamide (14). Benzoyl chloride (100 μL, 0.86 mmol) was dissolved in anhydrous THF (5 mL) under argon. Cyclohexanemethylamine (1.027 equiv) and TEA (2.5 equiv) were added, accompanied by formation of a white precipitate. After stirring at room temperature for 15 h, the reaction mixture was filtered and the filtrate concentrated. Pure amide **14** (155 mg, 83%) was isolated following chromatography (3:6:1 CHCl₃:hexanes:EtOAc): mp 109–110 °C; IR (KBr) 3344, 2914, 2847, 1636, 1548, 1492, 1442 cm⁻¹; ¹H NMR (500 MHz, CDCl₃) δ 7.760 (d, 2 H, *J* = 7.0 Hz), 7.490 (m, 1 H), 7.427 (m, 2 H), 6.168 (br s, 1 H, amine), 3.307 (t, 2 H, *J* = 6.5 Hz), 1.82–1.72 (m, 4 H), 1.70–1.65 (m, 1 H), 1.63–1.55 (m, 1 H), 1.30–1.13 (m, 3 H), 1.05–0.95 (m, 2 H); HRMS (EI) calcd for C₁₄H₁₉N₁O₁ 217.1467, found 217.1466.

(28) Merkushev, E. B.; Yudina, N. D. *Zh. Org. Khim.* 1982, 17, 2598–2601.

(29) Askew, B.; Ballester, P.; Buhr, C.; Jeong, K. S.; Jones, S.; Parris, K.; Williams, K.; Rebek, J., Jr. *J. Am. Chem. Soc.* 1989, 111, 1082–1090.

Pentafluorophenyl-2-Naphthoate (15). Pentafluorophenol (1.04 equiv) was added to a solution of 2-naphthoyl chloride (218 mg, 1.14 mmol) in anhydrous THF (10 mL). Triethylamine (1.25 equiv) was added to the solution, accompanied by the formation of a white precipitate. After stirring at room temperature for 21 h, the reaction was filtered to remove TEA·HCl, and the filtrate was concentrated. The pure (>97% by HPLC) active ester **15** (238 mg, 61%) was isolated as a white solid by chromatography (10% CHCl₃/hexanes): mp 92.9–93.7 °C; ¹H NMR (500 MHz, CDCl₃) δ 8.816 (s, 1H), 8.163 (dd, 1H, *J* = 8.5, 1.5 Hz), 8.024 (d, 1H, *J* = 8.0 Hz), 7.986 (d, 1H, *J* = 8.5 Hz), 7.944 (d, 1H, *J* = 8.5 Hz), 7.683 (d, 1H, *J* = 7.5 Hz), 7.619 (t, 1H, *J* = 7.5 Hz).

5'-((2-Naphthyl)carbonyl)amino)-5'-deoxy-2',3'-isopropylideneadenosine (16). Aminoadenosine **2** (51 mg, 0.166 mmol) and 2-naphthoyl chloride (1.17 equiv) were dissolved in anhydrous THF (10 mL) with an excess of TEA (8.6 equiv) under Ar, accompanied by the immediate formation of a white precipitate. The reaction was stirred at room temperature for 15 h, and filtered to remove TEA·HCl. After concentration, the residue was purified by flash chromatography (5% MeOH/CHCl₃) to yield **16** (76.6 mg, 99%) as a white powder: mp 145–150 °C dec; IR (KBr) 3322, 3172, 2928, 1644, 1598, 1533, 1474 cm⁻¹; ¹H NMR (250 MHz, DMSO-*d*₆) δ 8.836 (t, 1H, *J* = 5.5 Hz), 8.433 (s, 1H), 8.346 (s, 1H), 8.073 (s, 1H), 8.03–7.88 (m, 4H), 7.65–7.55 (m, 2H), 7.355 (br s, 2H, amine), 6.166 (d, 1H, *J* = 2.8 Hz), 5.500 (dd, 1H, *J* = 6.3, 2.8 Hz), 5.091 (dd, 1H, *J* = 6.3, 3.3 Hz), 4.351 (m, 1H), 3.588 (m, 2H), 1.530 (s, 3H), 1.314 (s, 3H); HRMS (EI) calcd for C₂₄H₂₄N₆O₄ 460.1859; found 460.1862.

Spectroscopy. Dilution and variable-temperature ¹H NMR studies were performed at 500 MHz using Varian VXR-500 NMR spectrometers equipped with Oxford VTC-4 temperature controllers and 5 mm direct or indirect detection ¹H/¹⁹F probes. Temperatures are not calibrated. DMSO-*d*₆ (99.9%-D), THF-*d*₈ (99.5%-D), and "100%" CDCl₃ (99.96%-D) were supplied by Cambridge Isotope Labs.

Titrations. ¹H NMR titrations were performed at 298 K at 300 MHz on a Varian UN-300 instrument with a 5 mm ¹H/¹⁹F/broad band probe and an Oxford VTC-4 temperature controller (THF-*d*₈) or at 500 MHz on a Varian VXR-500 instrument with a 5 mm ¹H/¹⁹F indirect detection probe and an Oxford VTC-4 temperature controller (CDCl₃).

In THF-*d*₈ (99.5%-D, CIL), the imide proton was followed through a 3.22 ppm downfield change in chemical shift as 2',3'-isopropylideneadenosine (10 mM) was added to a 2 mM solution of diimide **9** (700 μL). In CDCl₃ (99.8%-D, CIL), the upfield shift of adenine aromatic protons was monitored as a solution of **9** (2 mM) was added to 2',3'-isopropylideneadenosine (1 mM).

Comparison of the resonances of **12** from 0.068 mM to 19.41 mM in DMSO-*d*₆ show the following chemical shift changes: (i) downfield shift of the imide proton, (ii) upfield shifts of the adenine C²H and C⁸H protons, (iii) downfield shift of carbazole C⁴H, (iv) downfield shifts of the adenine NH₂ protons, and (v) upfield shifts of the ribose 1' and 2' protons. Though the magnitude of the changes is very small (~0.01 ppm), these chemical shifts are typical of adenine binding within the diimide pocket, bound on top of the carbazole and biphenyl surfaces.

Association constants were calculated by nonlinear least-squares regression fit of the data to the 1:1 binding isotherm using Systat 5.2.³⁰ The final chemical shift and association constant were treated as variables; the experimental value for the initial chemical shift was used.

Molecular Modeling. Predicted structures were generated by molecular mechanics minimization on a Silicon Graphics 4D30G+ Personal Iris running MacroModel 3.5X³¹ using a modified AMBER³² force field (AMBER*) and the truncated Newton conjugate gradient algorithm³³ (TNCG) to the default gradient of less than 0.05 kJ/Å. Chloroform solution was simulated using the Generalized Born/Surface Area method (GB/SA).³⁴ The autocatalytic tetrahedral intermediate was generated by minimization of the O-protonated, N-deprotonated neutral tautomer using the Polak-Ribiere³⁵ conjugate gradient algorithm and the AMBER* force field to a low energy gradient (8.91 × 10⁻⁴ kJ/mol-Å).

Kinetic Studies. All reactions were performed at 6.2 mM initial concentrations of reactants in 13% THF/CHCl₃ with 1.0% TEA base. A THF stock solution of 5'-amino-5'-deoxy-2',3'-isopropylideneadenosine (**2**) was prepared daily. All other solutions were freshly prepared for each kinetic run. Formation of products was followed by HPLC at 270 nm on a Waters 600E instrument equipped with a Waters 717 autosampler and a Waters 490E UV detector. Temperature inside the autosampler was constant at 22 ± 1 °C in an individually thermostated room. Product formation was followed for the first 5–10% of the reaction; initial rates were determined by linear fitting of the absolute size of the product peak areas. Kinetic runs showed excellent linearity (*R*² > 0.990) and good convergence to the origin (except in runs where product was added at time = 0). HPLC separation was achieved using a Beckman Ultrasphere SI column (4.6 mm i.d. × 25 cm length). The elution system was 1% MeOH/CHCl₃, 1.5 mL/min to 3.0 mL/min over 5 min; then 5% MeOH/CHCl₃, 4 mL/min for 8 min. Under these conditions, the retention times of ester **11** and product **12** were 2.1 and 8.2 min, respectively. Aminoadenosine **2** was retained on the column and removed by flushing the column with 1/10/89% TEA/MeOH/CHCl₃ after each experiment (usually 6–8 injections).

Acknowledgment. We are grateful to the National Science Foundation for financial support. E.A.W. thanks the NSF and M.M.C. the NSERC for predoctoral fellowships. This research was supported by the National Science Foundation.

(30) Systat 5.2, Systat Inc., Evanston, Ill, 1992.

(31) Mohamadi, F.; Richards, N. G.; Guida, W. C.; Liskamp, R.; Lipton, M.; Cauffield, C.; Chang, G.; Hendrickson, T.; Still, W. C. *J. Comput. Chem.* **1990**, *11*, 440–467.

(32) Weiner, S. J.; Kollman, P. A.; Case, D.; Singh, U. C.; Alagona, G.; Profeta, S.; Weiner, P. *J. Am. Chem. Soc.* **1984**, *106*, 765–784.

(33) Ponder, J. W.; Richards, F. M. *J. Comput. Chem.* **1987**, *8*, 1016–1024.

(34) Still, W. C.; Tempczyk, A.; Hawley, R. C.; Hendrickson, T. *J. Am. Chem. Soc.* **1990**, *112*, 6127–6129.

(35) Polak, E.; Ribiere, G. *Revue Française Inf. Rech. Oper.* **1969**, *16*, 35.